Multiscale modeling of the iron *bcc* → *hcp* martensitic phase transformation

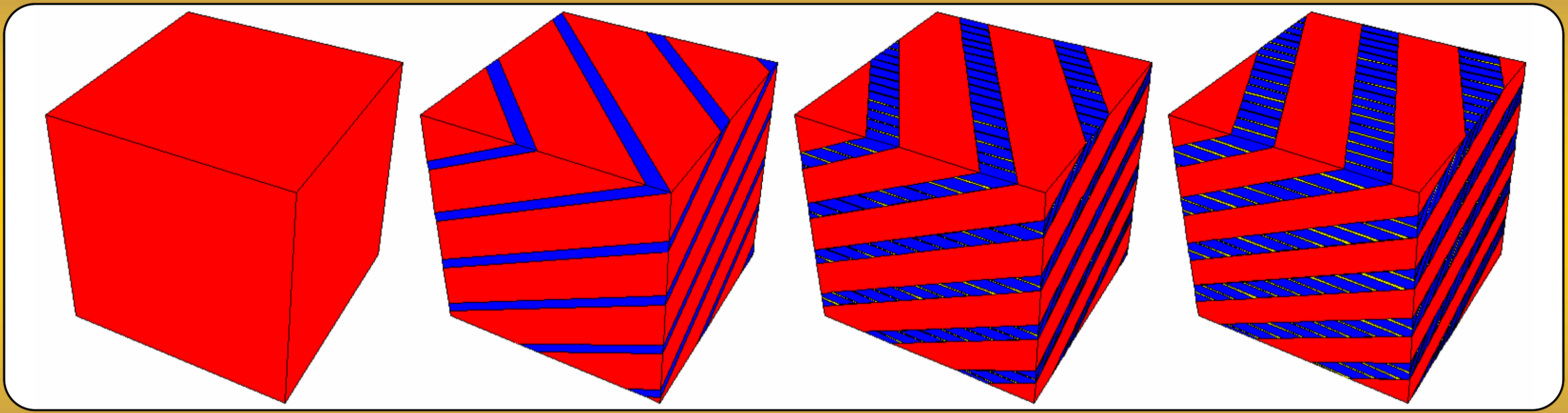

Kyle J. Caspersen and Emily Carter
Department of Chemistry and Biochemistry
University of California Los Angeles

Adrian Lew* and Michael Ortiz
Graduate School of Aeronautics
California Institute of Technology

Funded by the Department of Energy - Accelerated Strategic Computing Initiative (DOE-ASCI)

*Stanford University

Iron Properties

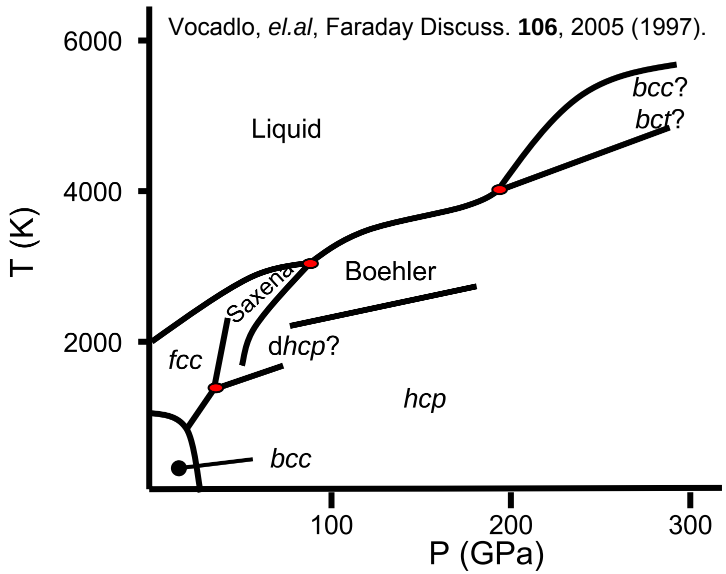

Ground state ferromagnetic *bcc* undergoes a *martensitic* phase transformation to non-magnetic *hcp* at ~10 GPa.

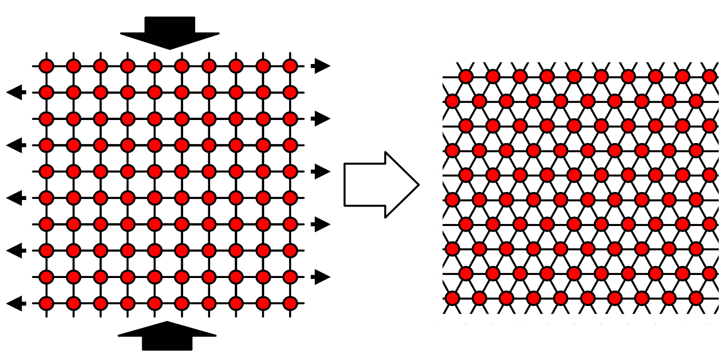

A strong shock wave will induce phase transitions producing complicated microstructure.

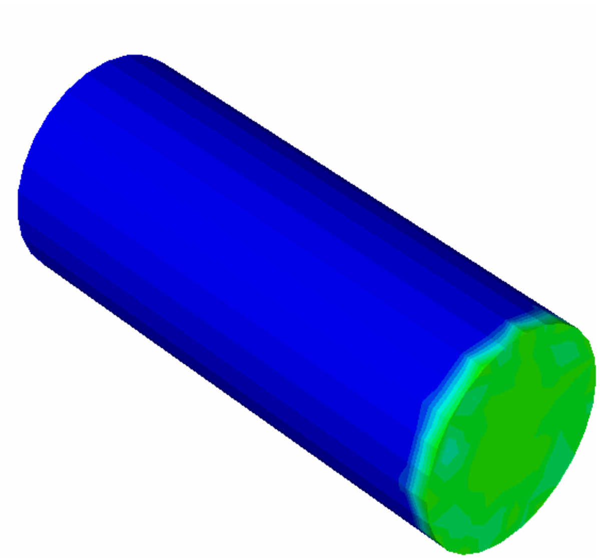

- considerable scatter in the measured transformation pressures
- large hysteresis

Goal: understand scatter and hysteresis in transition pressures

Iron Properties

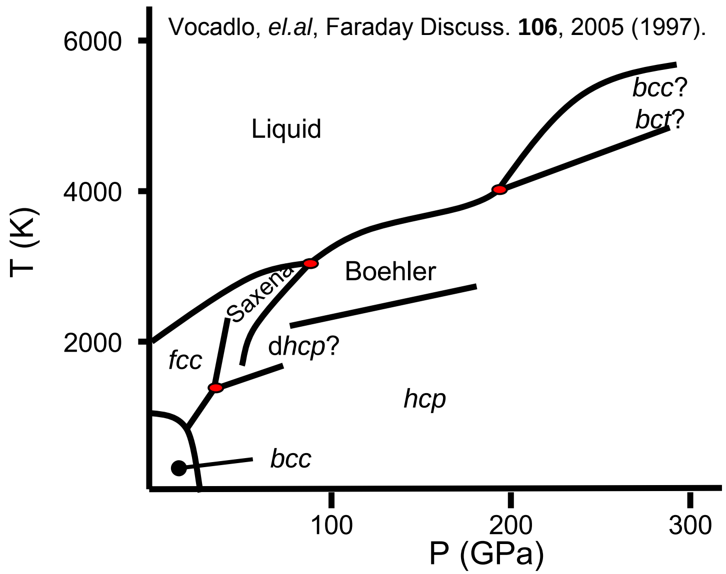

A strong shock wave will induce phase transitions producing complicated microstructure.

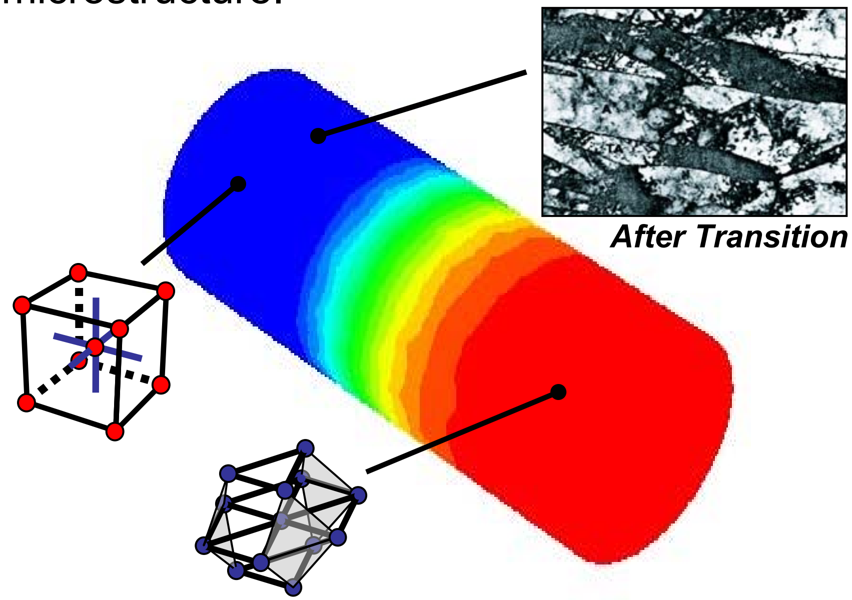

Ground state ferromagnetic *bcc* undergoes a *martensitic* phase transformation to non-magnetic *hcp* at ~10 GPa.

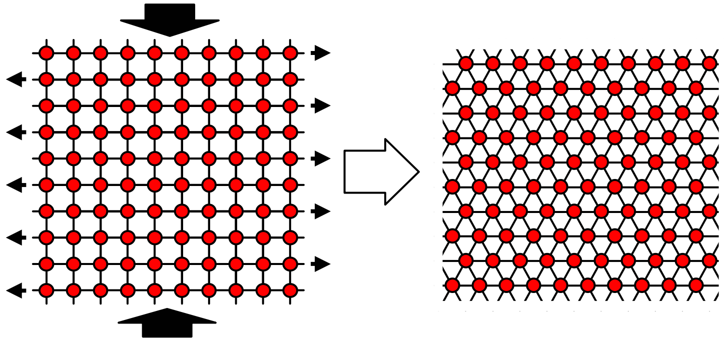

- considerable scatter in the measured transformation pressures
- large hysteresis

Goal: understand scatter and hysteresis in transition pressures

Phase Mixing

Constrained Two State System

- fixed amount in confined volume
- particles can be one of two phases

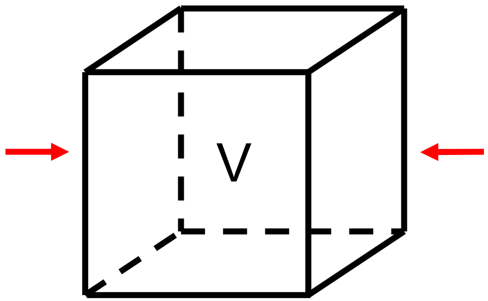

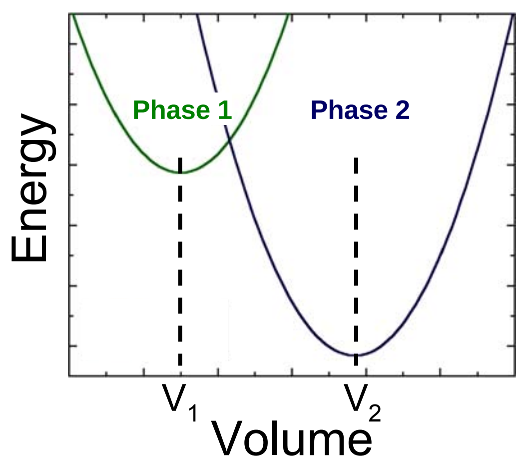

What is the composition for any V?

Mixed Two State System

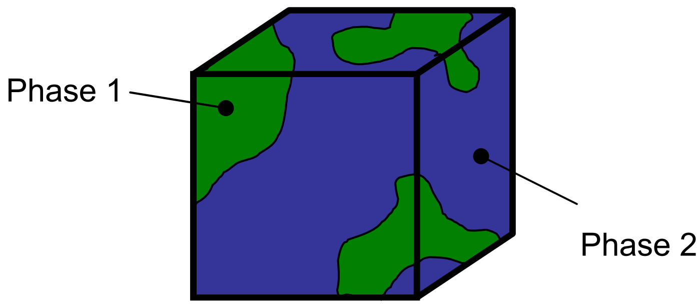

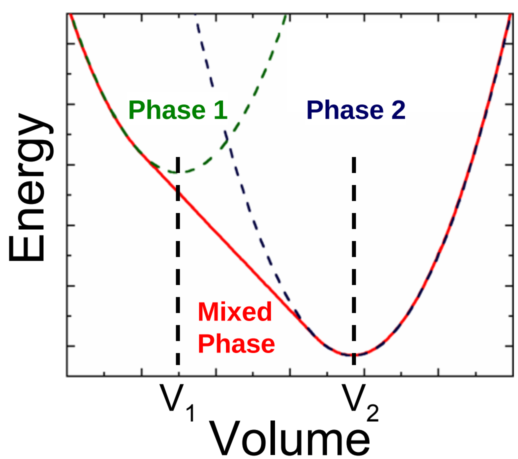

Gibbs construction – equation of state is given by drawing the line of common tangent

Mixing lowers the total system energy

Sequential Laminates

- a combination of layers composed of different uniform deformations (F), provided

$$V_{tot} = \sum_i V_i$$

$$\boldsymbol{F}_{tot} = \sum_i \boldsymbol{F}_i$$

V = Volume
F = Deformation

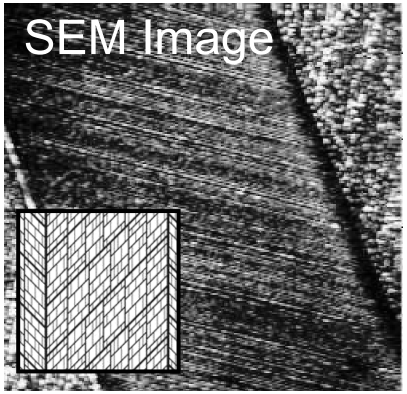

- layers composed of alternating phases
  - Simple Laminate : two layers, rank 1
  - Sequential Laminate : laminate of laminates, hierarchy of length scales

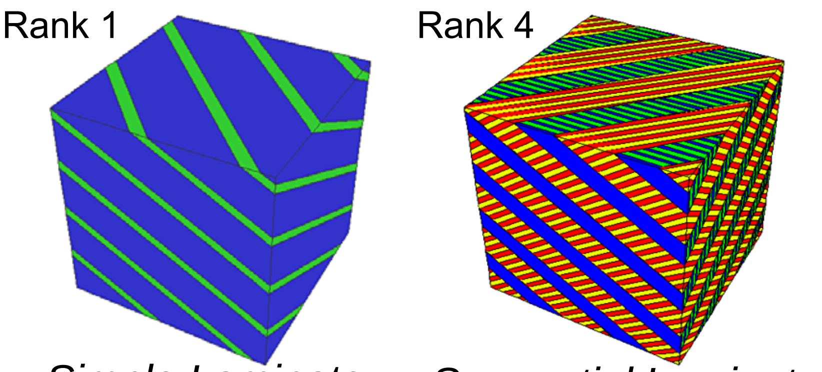

Simple Laminate *Sequential Laminate*

- laminate must be kinematically compatible
  - obey the Hadamard compatibility condition

$$\boldsymbol{F}_1 - \boldsymbol{F}_2 = \boldsymbol{a} \otimes \boldsymbol{n}$$

  - no slip or gaps

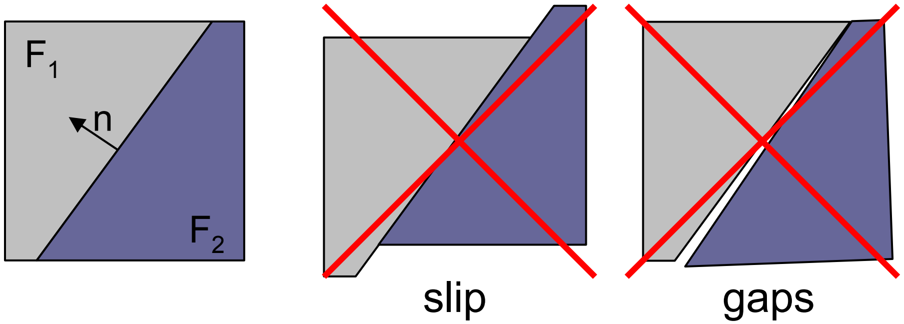

Multiscale Iron Model

The model treats iron as laminates, not as single crystals

- **layers consist of *bcc* or *hcp* crystallite that minimizes the energy (W)**

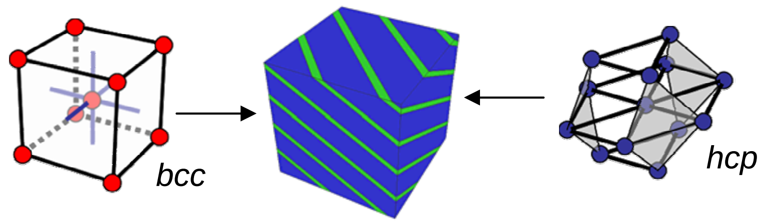

$$W(\boldsymbol{F}) = \min_{i=0,\ldots,N-1} W^i(\boldsymbol{F})$$

- **allowed crystallites depend on transformation path**

  variant – an allowed bcc or hcp crystallite
  with a specific orientation

  - initially the crystal is a single grain
  - variants formed through a phase transformation

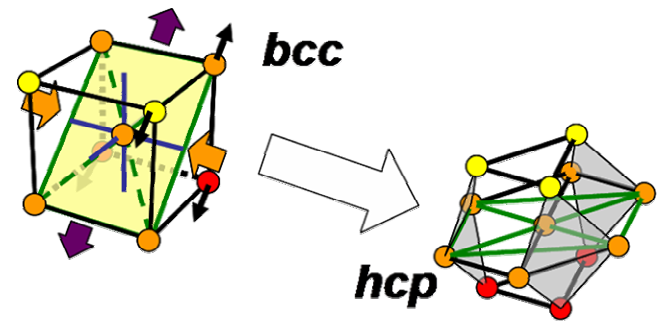

- ***F*s obey the Hadamard compatibility condition**
  - this condition makes the problem non-trivial
  - precludes direct optimization of volume fractions via the Gibbs construction (which ignores this condition)
  - S. Aubry, M. Fago, and M. Ortiz, Computer Methods in Applied Mechanics and Engineering **192**, 2823 (2003).

$$\boldsymbol{F}_1 - \boldsymbol{F}_2 = \boldsymbol{a} \otimes \boldsymbol{n}$$

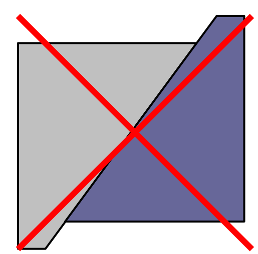

slip

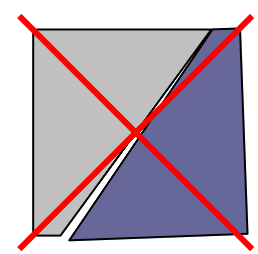

gaps

bcc → *hcp* Phase Transformation

Burgers' path

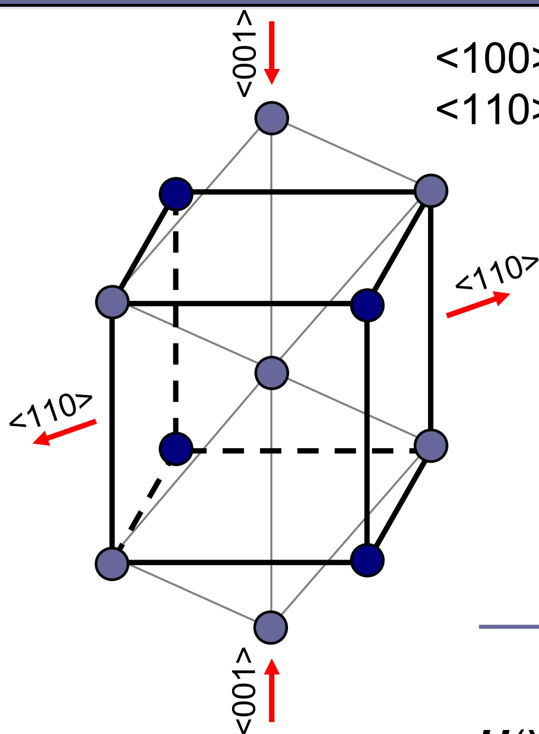

<100> compression
<110> elongation

$\xrightarrow{\boldsymbol{U}}$

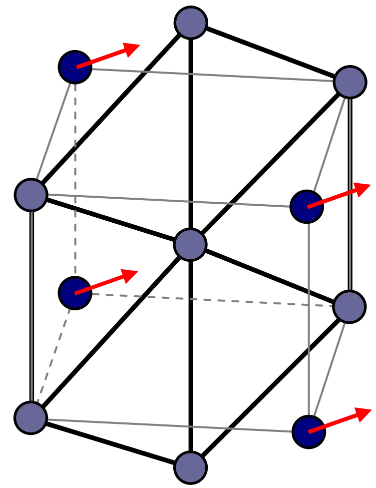

<110> shuffle

$\xrightarrow{\boldsymbol{u}}$

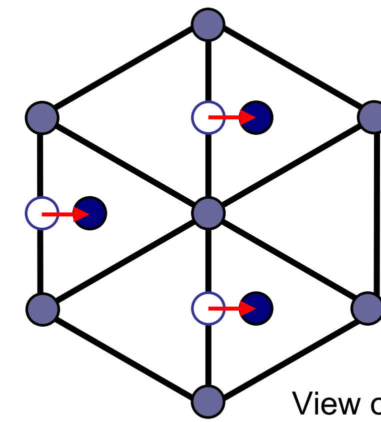

View of
<110> Plane

$$\boldsymbol{U}(\mathrm{V}) = \begin{pmatrix} \frac{\alpha(\mathrm{V})}{2} + \frac{3}{4\sqrt{2}} & \frac{\alpha(\mathrm{V})}{2} - \frac{3}{4\sqrt{2}} & 0 \\ \frac{\alpha(\mathrm{V})}{2} - \frac{3}{4\sqrt{2}} & \frac{\alpha(\mathrm{V})}{2} + \frac{3}{4\sqrt{2}} & 0 \\ 0 & 0 & \frac{\sqrt{3}}{2} \end{pmatrix} \qquad \boldsymbol{u} = \begin{pmatrix} \frac{1}{4\sqrt{2}} \\ \frac{-1}{4\sqrt{2}} \\ 0 \end{pmatrix}$$

- ***U*** is an *hcp* deformation
- ***u*** is the shuffle
- $\alpha(\mathrm{V}) = \sqrt{3/8}\,(c/a)_{\mathrm{V}}$

initial *bcc* variant

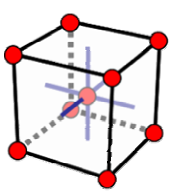

G ∈ *bcc* point group

$\xrightarrow{\boldsymbol{UG}}$

6 *hcp* variants

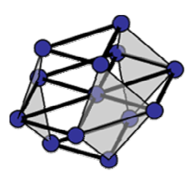

H ∈ *hcp* point group

$\xrightarrow{\boldsymbol{G^{-1}U^{-1}HUG}}$

12 *bcc* variants

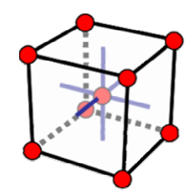

19 total variants

Variant Energy

$$W(\boldsymbol{F}) = \min_{i=0,\ldots,18} W^{i}(\boldsymbol{F})$$

DFT calculations prove to costly for on-the-fly W(*F*) or tabulated W(*F*)

Assumption: each deformation close to deformation of a variant

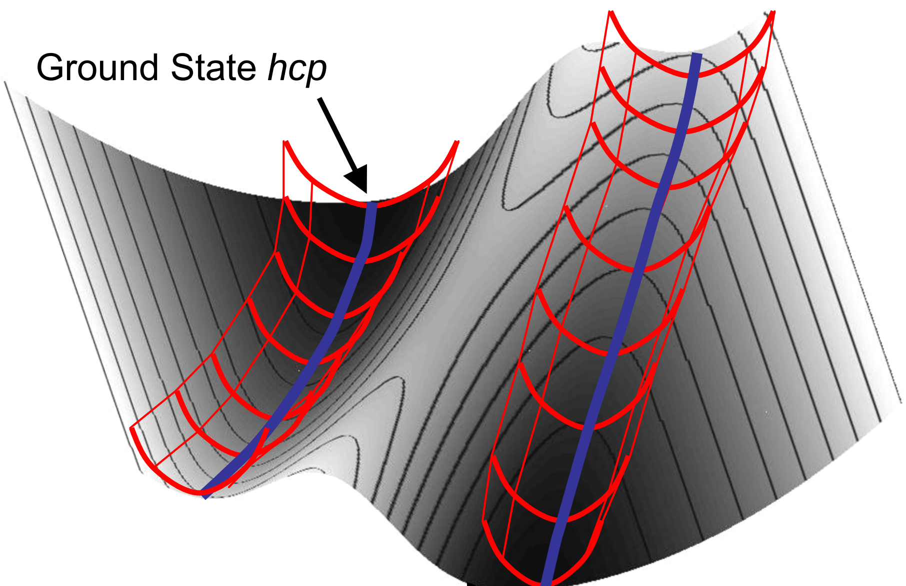

Approximation: Taylor expansion around variant deformation

Taylor Expansion

$$W^{i}(\boldsymbol{C}) = W^{i}_{0}(V) + \tfrac{1}{2}\left(\boldsymbol{C} - \boldsymbol{C}^{i}(V)\right)^{T} \boldsymbol{\Gamma}^{i}(V)\left(\boldsymbol{C} - \boldsymbol{C}^{i}(V)\right)$$

$$\boldsymbol{\Gamma}^{i}(V) = \left.\frac{\partial^{2} W^{i}}{\partial \boldsymbol{C}^{2}}\right|_{\boldsymbol{C}^{i}(V)} \qquad \boldsymbol{C} = \boldsymbol{F}^{T}\boldsymbol{F}$$

DFT Calculations

- Variant deformation, $\boldsymbol{C}^{i}(V)$ (*hcp* c/a ratio)
- Equation of State, $W^{i}_{0}(V) = W^{i}(\boldsymbol{C}^{i}(V))$
- Non-Linear Elastic Constants, $\boldsymbol{\Gamma}^{i}(V)$ (Calculated using volume conserving shears)

bcc and *fcc* : $\Gamma_{11}\ \Gamma_{12}\ \Gamma_{44}$

hcp : $\Gamma_{11}\ \Gamma_{33}\ \Gamma_{12}\ \Gamma_{13}\ \Gamma_{44}$

DFT Details

- Kohn-Sham DFT within VASP
- GGA and PW-91
- Projector Augmented Wave (PAW) all electron method
- 2 Ions/Cell
- 24×24 ×24 Monkhorst Pack K-Point Grid
- 500 eV Kinetic Energy Cut Off
- Spin-Polarized for *bcc*

First Principles Input

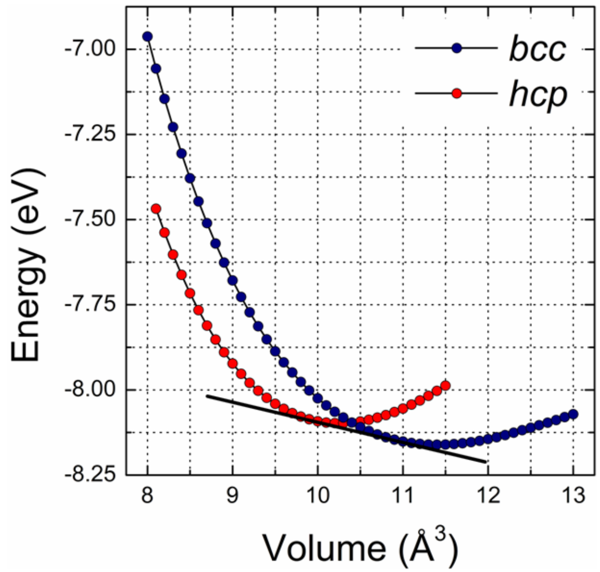

bcc→*hcp*	Transition Pressure (GPa)
EXPERIMENT	10-15
FLAPW*	11.5
PAW	10

- PAW predicts the *bcc* to *hcp* transition pressure within the measured range

* Herper, et.al, Phys. Rev. B **60**, 3839 (1999).

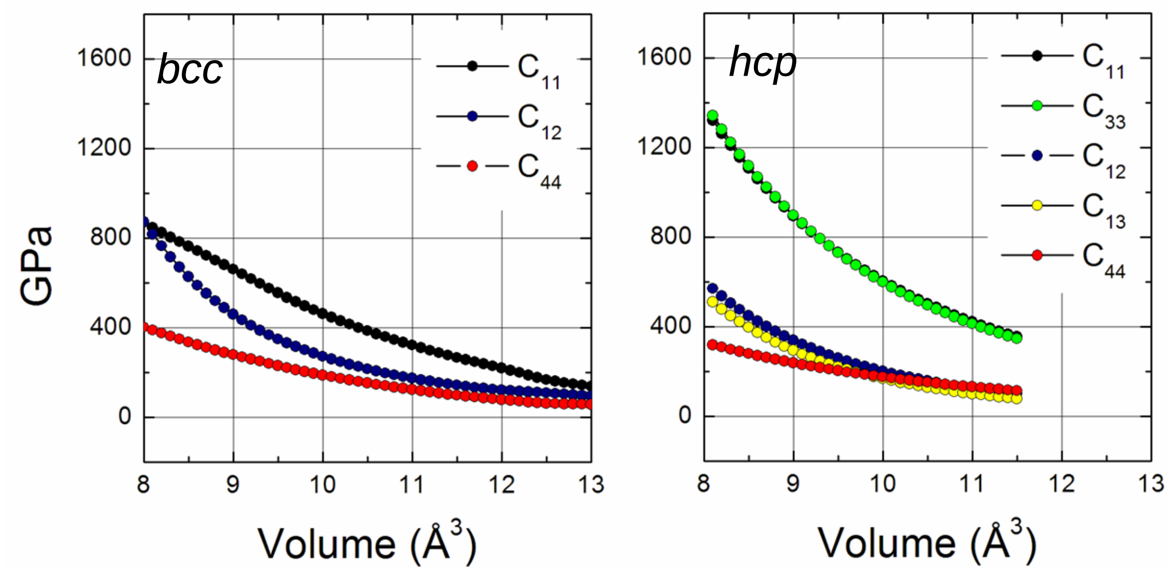

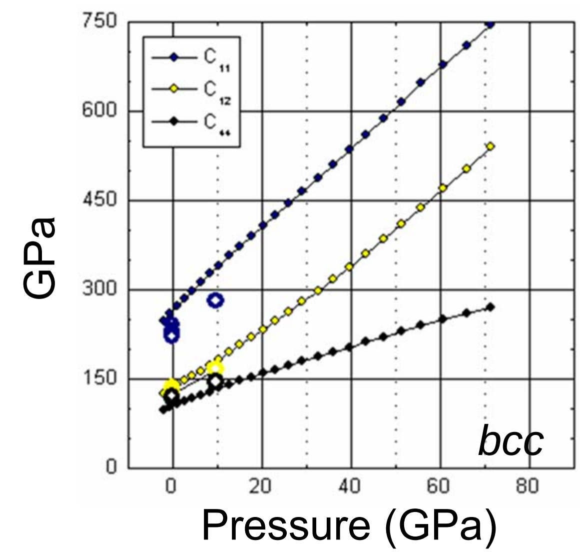

- *bcc* elastic constants compare well with experiment (C_{11} a bit high)
- little experimental data for *hcp*

Compression

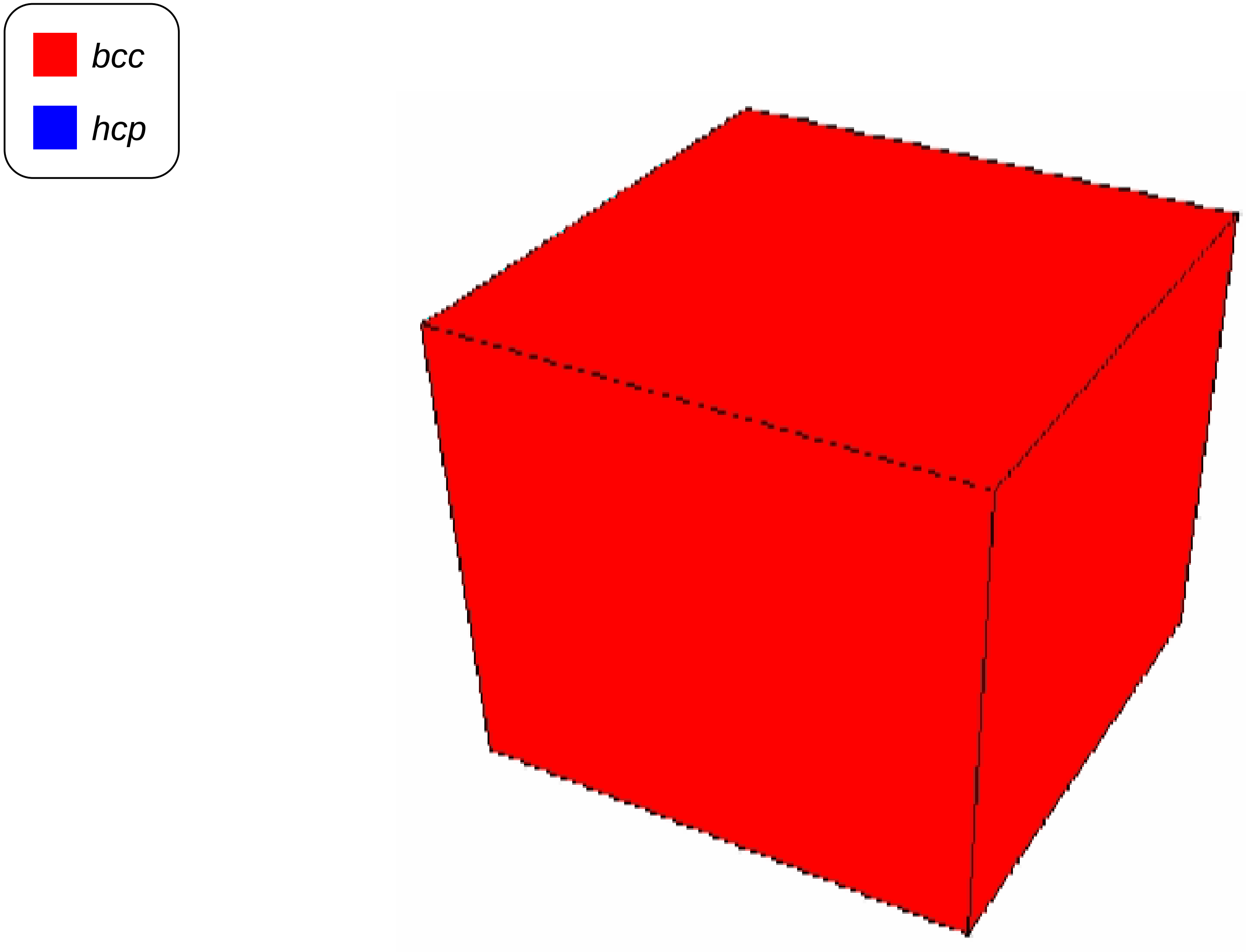

Shear Compression

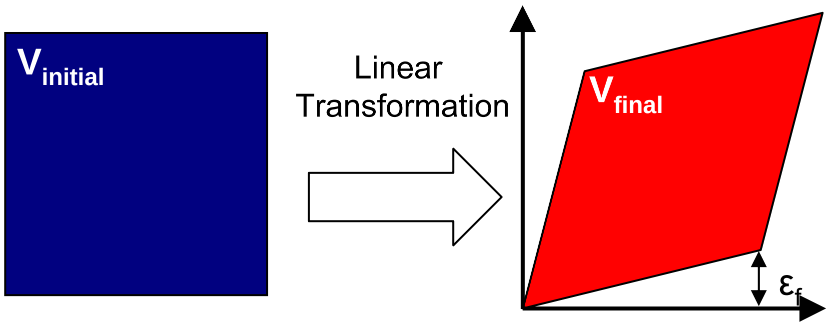

$$\boldsymbol{F}(\delta) = (1-\delta)\begin{pmatrix} 1 & 0 & 0 \\ 0 & 1 & 0 \\ 0 & 0 & 1 \end{pmatrix} + \delta\begin{pmatrix} \lambda & \varepsilon_f & 0 \\ \varepsilon_f & \lambda & 0 \\ 0 & 0 & \lambda \end{pmatrix}$$

undeformed *bcc*

λ is set such that $V=V_f$

(Note: det[***F***]=V)

$\varepsilon_f = 0.03$

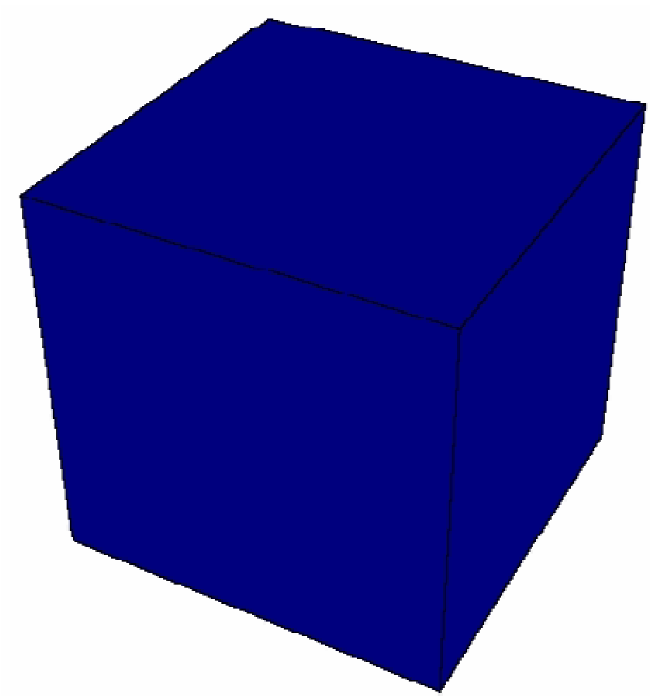

$\varepsilon_f = 0.04$

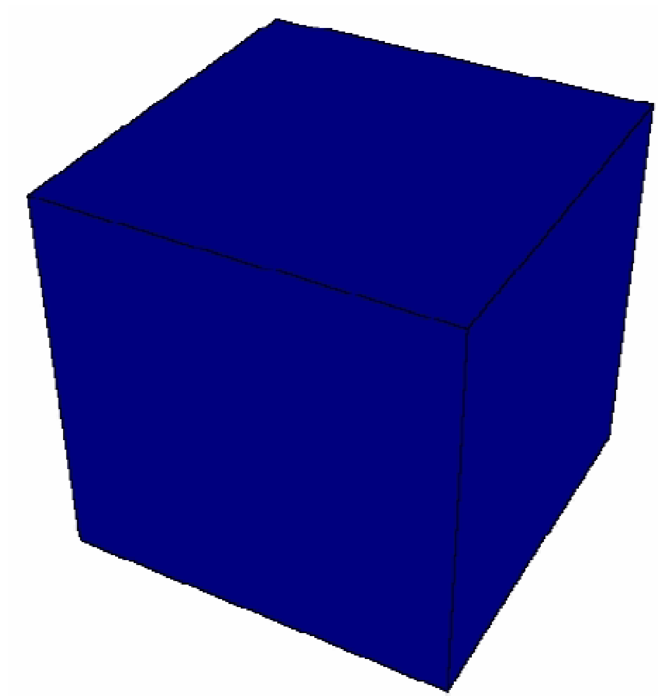

Note: mapped deformed volume onto reference volume

Role of Shear

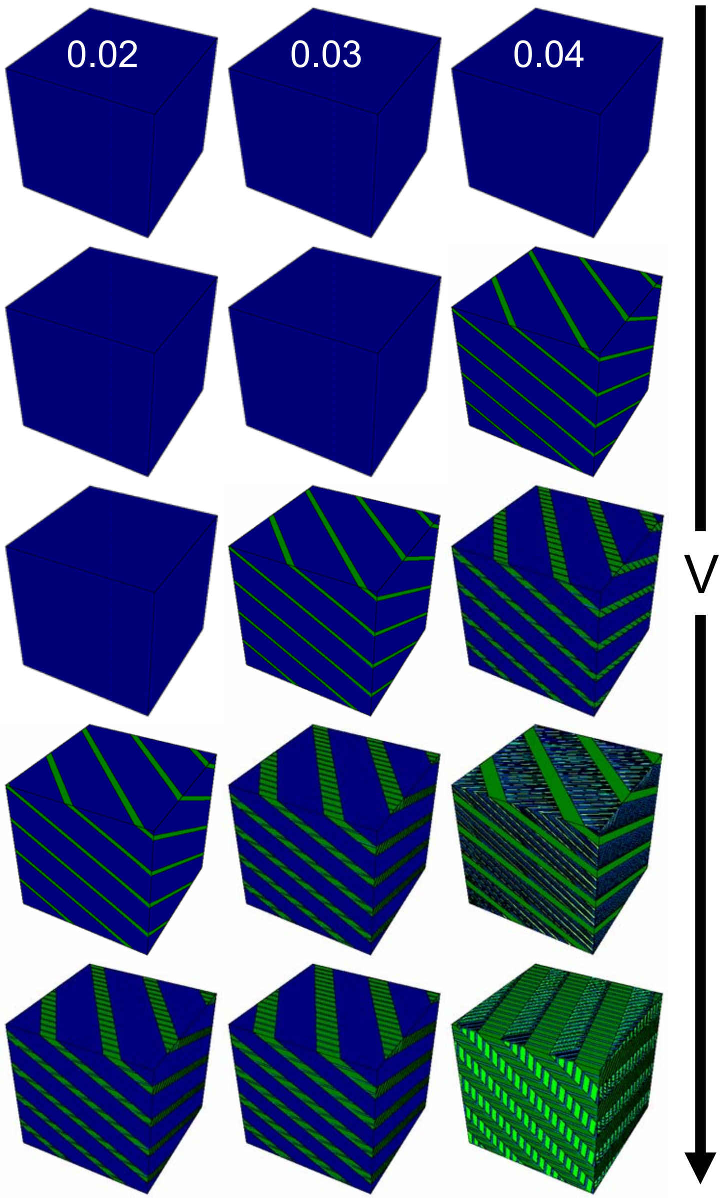

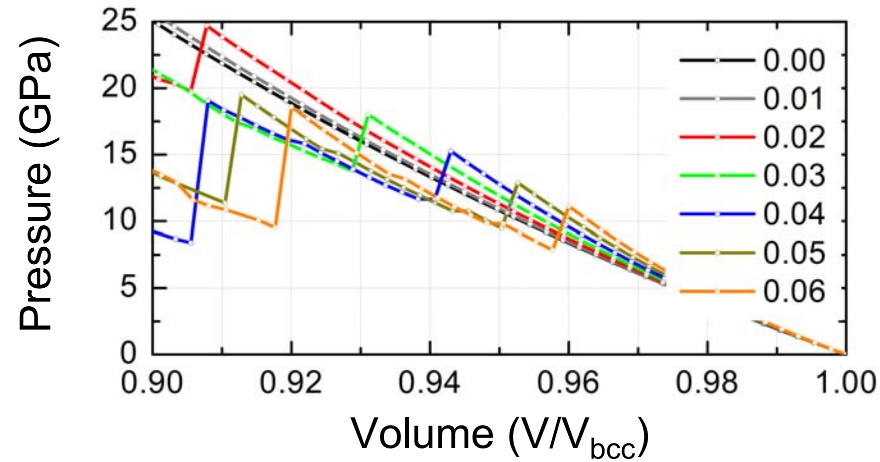

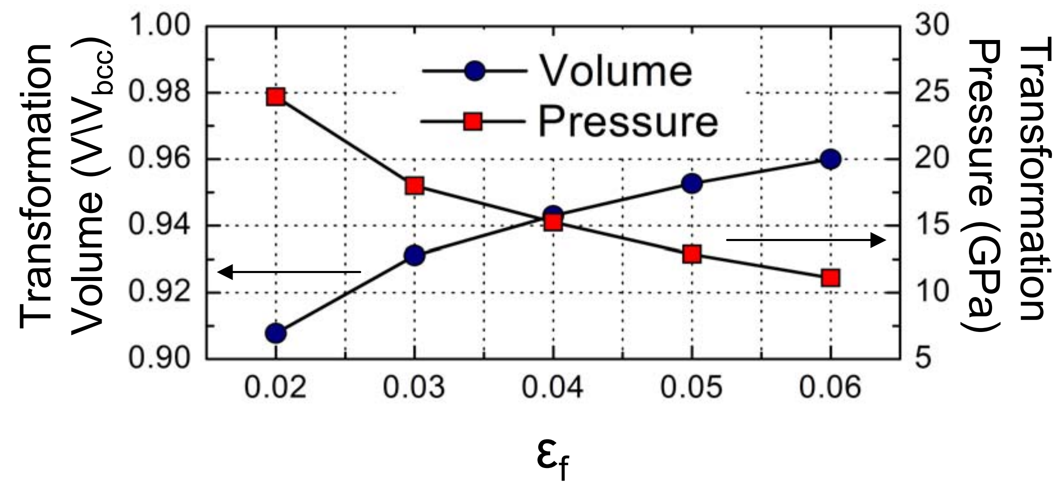

- shear is required to activate this transformation
- increasing shear lowers the TP and increases the TV
- variability in measured TPs may be due to shear states

bcc → *hcp* Phase Transformation

What are the average bulk properties of the bcc → hcp transformation?

To explore the transformation, we apply a series of volume-conserving deformations (F) along the transformation path.

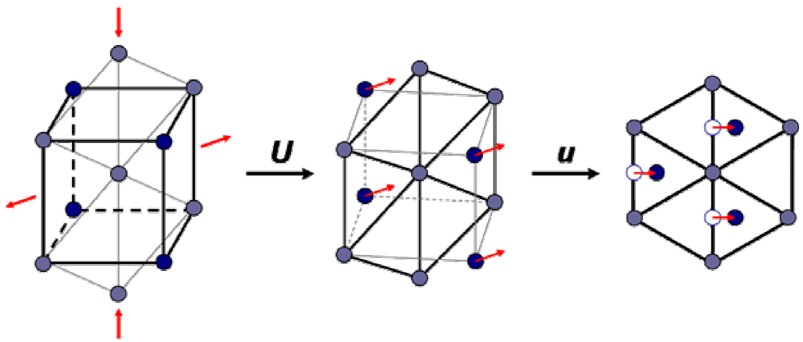

$$\boldsymbol{U}(\mathrm{V}) = \begin{pmatrix} \frac{\alpha(\mathrm{V})}{2} + \frac{3}{4\sqrt{2}} & \frac{\alpha(\mathrm{V})}{2} - \frac{3}{4\sqrt{2}} & 0 \\ \frac{\alpha(\mathrm{V})}{2} - \frac{3}{4\sqrt{2}} & \frac{\alpha(\mathrm{V})}{2} + \frac{3}{4\sqrt{2}} & 0 \\ 0 & 0 & \frac{\sqrt{3}}{2} \end{pmatrix}$$

$$\alpha(\mathrm{V}) = \sqrt{3/8}\,\left(c/a\right)_{\mathrm{V}}$$

bcc deformation

$$\boldsymbol{F}_{\mathrm{bcc}}(\mathrm{V}) = \mathrm{V}^{1/3}\,\boldsymbol{I}$$

hcp deformation

$$\boldsymbol{F}_{\mathrm{hcp}}(\mathrm{V}) = \left(\frac{\mathrm{V}}{\det \boldsymbol{U}(\mathrm{V})}\right)^{1/3} \boldsymbol{U}(\mathrm{V})$$

linear transformation

$$\boldsymbol{F}(\mathrm{V},\delta) = \omega_{\delta}\left[(1-\delta)\boldsymbol{F}_{\mathrm{bcc}}(\mathrm{V}) + \delta\,\boldsymbol{F}_{\mathrm{hcp}}(\mathrm{V})\right]$$

ω = volume-conserving scale factor

$0 \le \delta \le 1$

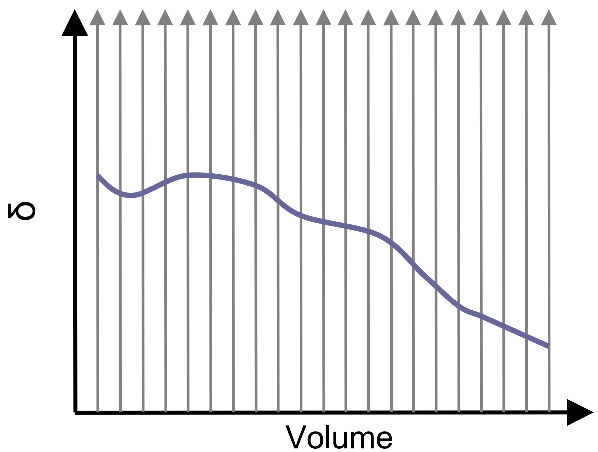

The F(V,δ) that minimizes W determines the transformation properties.

bcc → *hcp* Phase Transformation

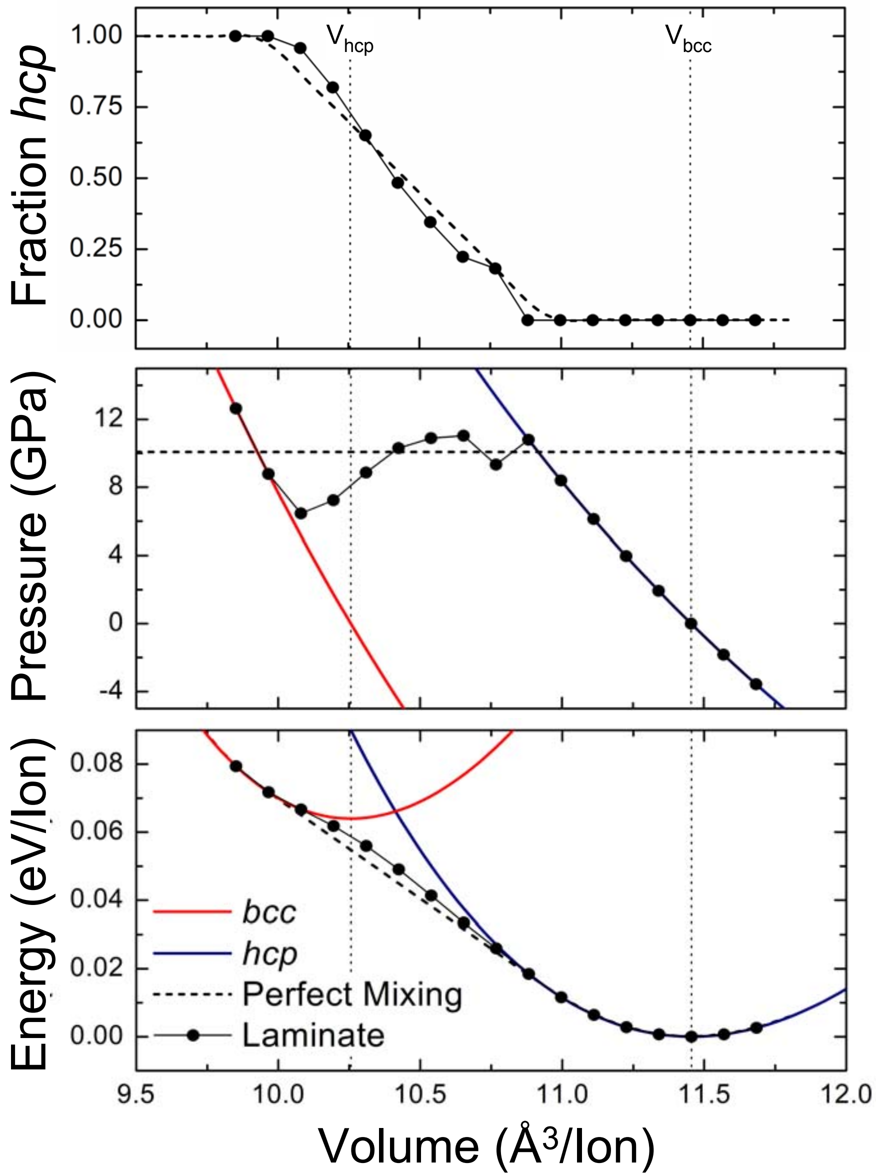

- **full conversion to *hcp***
- **transition pressure of 10 GPa**
- **hallmarks of Gibbs construction**
  - the lowering of the energy
  - the lag to full conversion to hcp
- **deviation from Gibbs construction**
  - no perfect tangent matching
  - energy is increased
  - caused by the two imposed constraints
    - Hadamard compatibility condition

$$\boldsymbol{F}_1 - \boldsymbol{F}_2 = \boldsymbol{a} \otimes \boldsymbol{n}$$

    - dependence on the transformation path

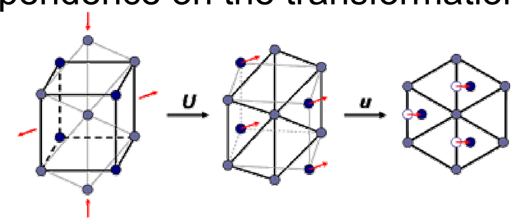

  - constraints introduce frustration
- **hysteresis width of ≈5.2 GPa observed**
  - loading TP = 10.2 GPa
  - unloading TP = 5.0 GPa
  - experimental width 6.2 GPa (Taylor et al.)

Directional Deformation of bcc Fe

- propagating shock waves apply load in specific directions

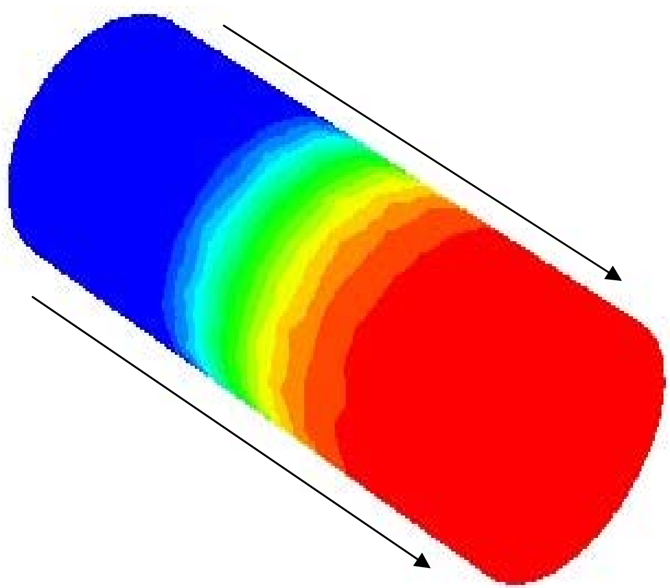

- what effect does the direction of applied load have on the transformation?

- to investigate directional loading we applied the directional deformation $\boldsymbol{F}_{\theta,\varphi}(\delta)$ spanning all direction space (angle space)

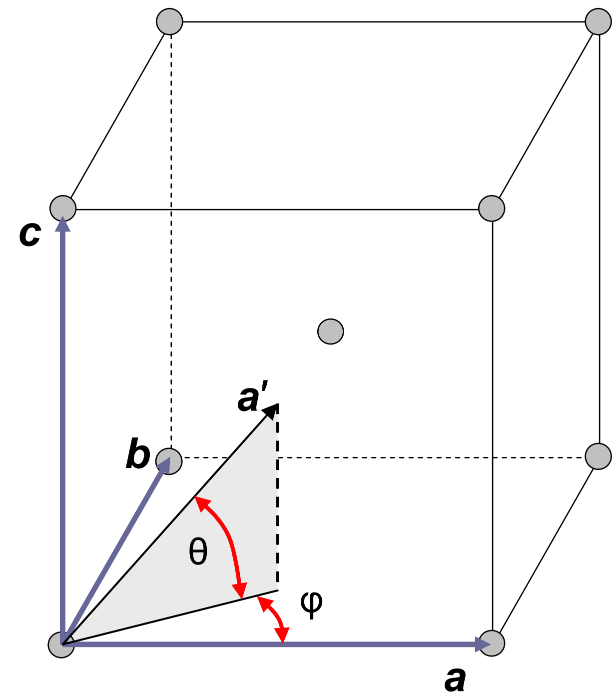

$$(\boldsymbol{a}',\boldsymbol{b}',\boldsymbol{c}') = \begin{pmatrix} \cos\varphi & \sin\varphi & 0 \\ -\sin\varphi & \cos\varphi & 0 \\ 0 & 0 & 1 \end{pmatrix} \begin{pmatrix} \cos\theta & 0 & \sin\theta \\ 0 & 1 & 0 \\ -\sin\theta & 0 & \cos\theta \end{pmatrix}$$

$$\boldsymbol{F}_{\theta,\varphi}(\delta) = \delta(\boldsymbol{a}' \otimes \boldsymbol{a}') + (\boldsymbol{b}' \otimes \boldsymbol{b}') + (\boldsymbol{c}' \otimes \boldsymbol{c}')$$

Directional Deformation of bcc Fe: TP and TV

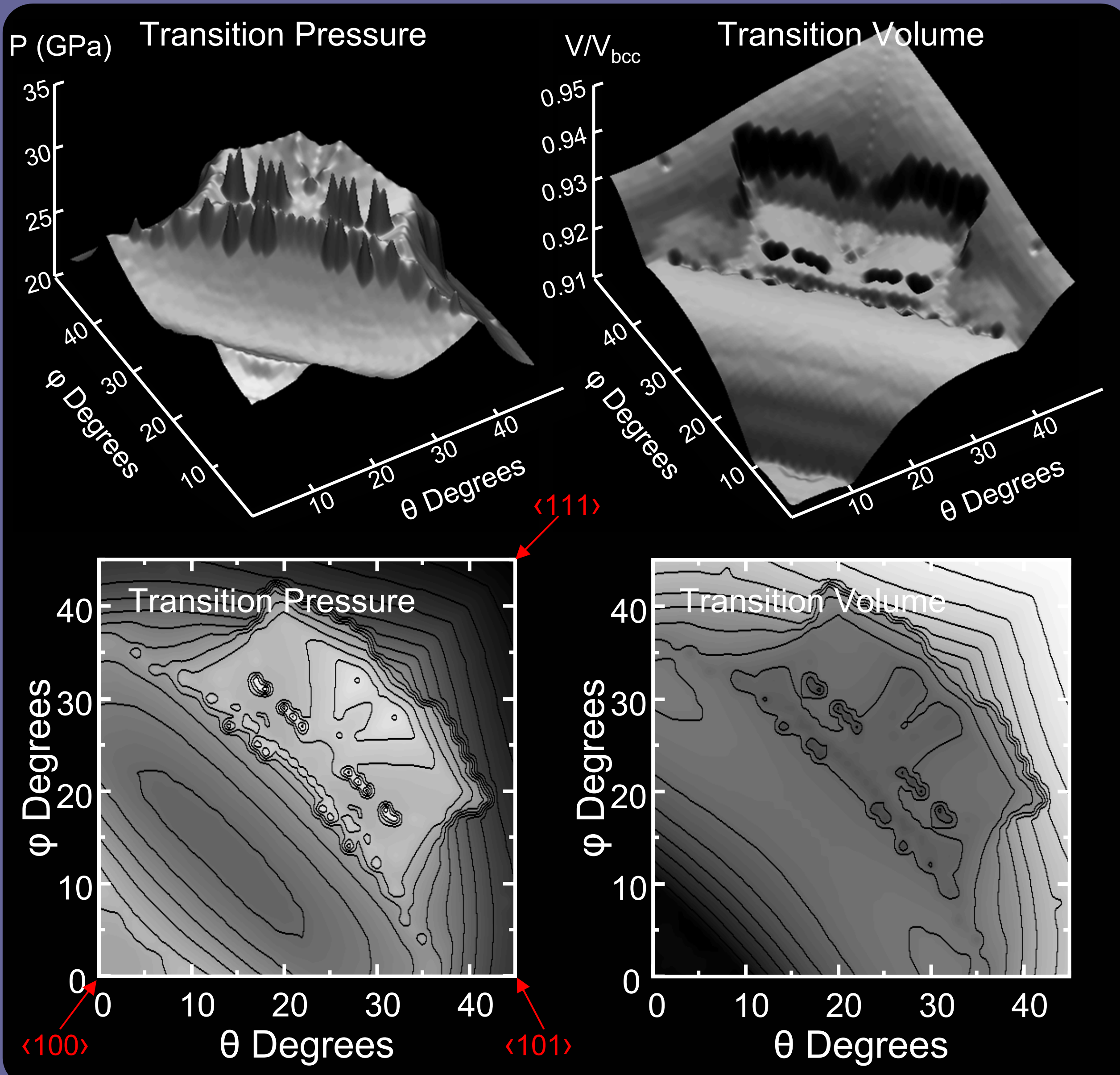

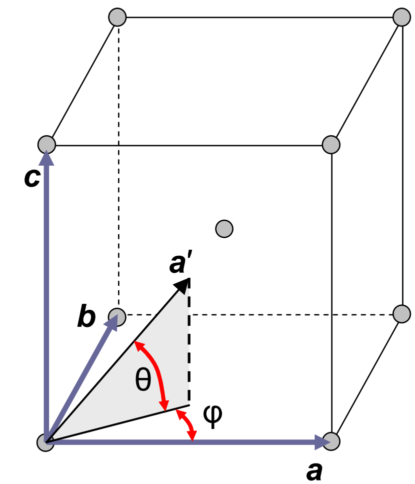

TP for all angles is high, >20 GPa
- never optimal combination of contraction and and shear

region of high pressure for moderate angles
- perhaps no hcp variant along path

loading parallel to simple facets facilitates the transformation
- notably the ‹110› planes

loading along the simple axes recovers smallest TP in that region of angle space
- ‹111›< ‹101›< ‹100›

Conclusions

Shear Compression

- shear is required for transformation to occur
- increasing shear lowers the TP and increases the TV
- sensitivity to shear may be responsible for the variability in the measured TPs

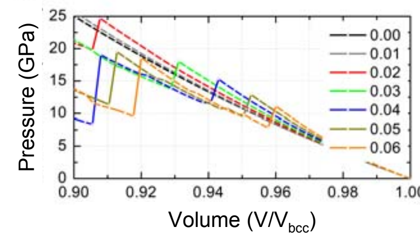

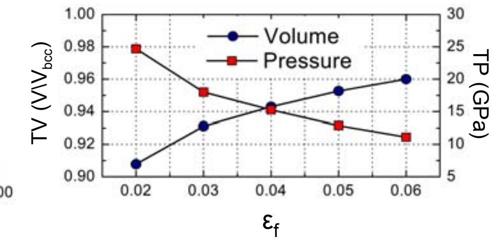

bcc-to-hcp Transformation

- full conversion to *hcp at* ≈10 GPa, consistent with the experimentally observed values
- hallmarks of the Gibbs construction
- deviation from "perfect" mixing due to imposed constraints
- shows hysteresis in the TP simply due to the crystalline kinematics

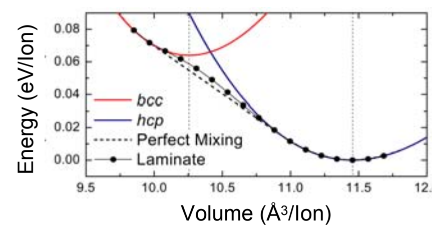

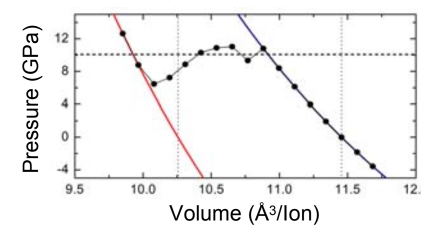

$$F_1 - F_2 = \boldsymbol{a} \otimes \boldsymbol{n}$$

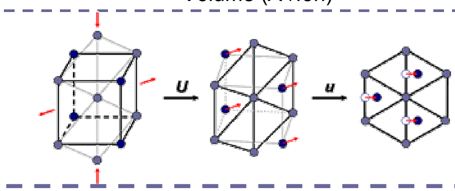

Directional Deformation

- transformation pressure is > 20GPa
- region of very high transformation pressure
- loading || to simple facets facilitates the transformation, in particular along simple axes

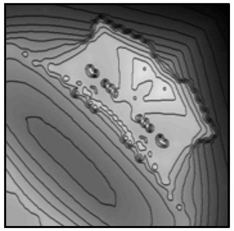

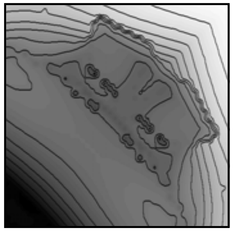

Acknowledgements

Matt Fago :S. Aubry, M. Fago, and M. Ortiz, Computer Methods in Applied Mechanics and Engineering **192**, 2823 (2003).
De-en Jiang
Robin Hayes
Emily Jarvis

Multiscale Modeling

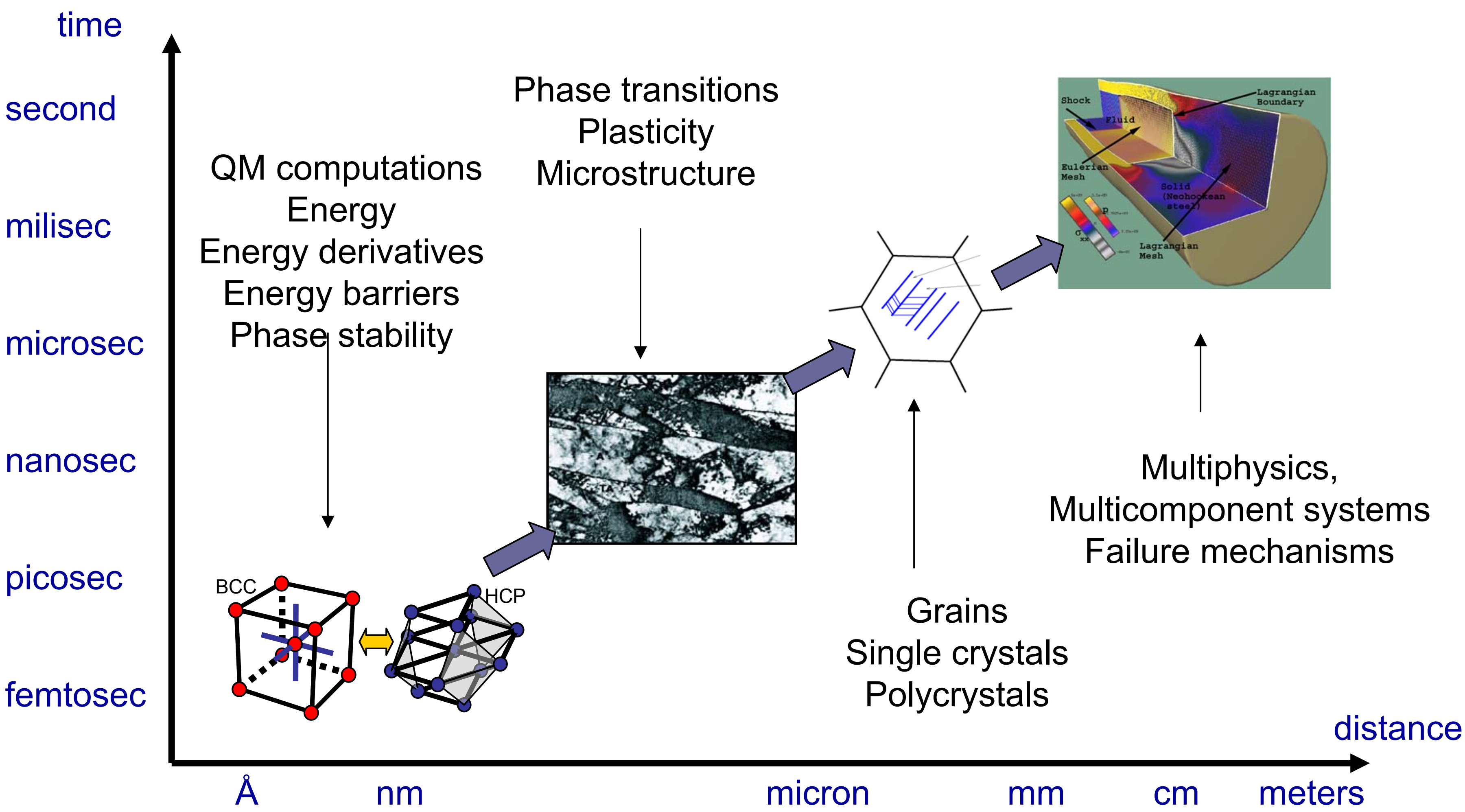

Calculated Equations of State

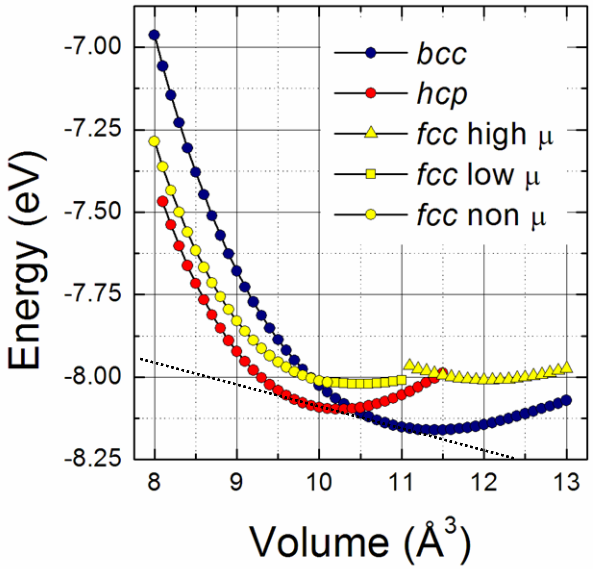

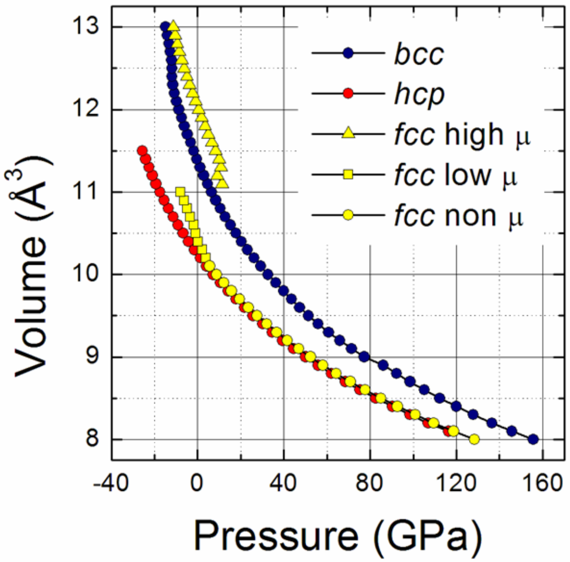

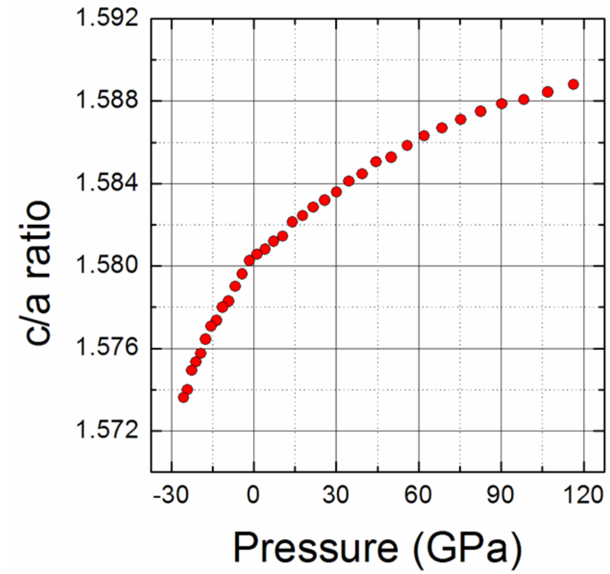

hcp	V_0 (Å^3)	K_0 (GPa)	c/a
EXPERIMENT	11.09	208	1.61
FLAPW	10.20	291	1.58
PAW	10.25	293	1.58

bcc	V_0 (Å^3)	K_0 (GPa)	μ
EXPERIMENT	11.69	172	2.22
FLAPW	11.40	174	2.17
PAW	11.43	172	2.21

bcc→*hcp*	Transition Pressure (GPa)
EXPERIMENT	10-15
FLAPW	11.5
PAW	10

- PAW reproduces the FLAPW results
- Both PAW and FLAPW do not compare well with experiments
  - Perhaps a problem with the extrapolation to T & P =0

- PAW reproduces the FLAPW results
- Both PAW and FLAPW compare reasonably well with experiments

- PAW predicts the observed *bcc* to *hcp* transition pressure

Calculated Elastic Constants

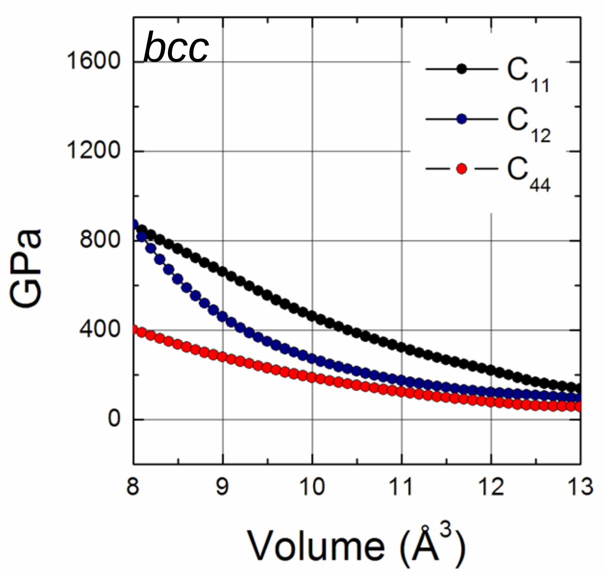

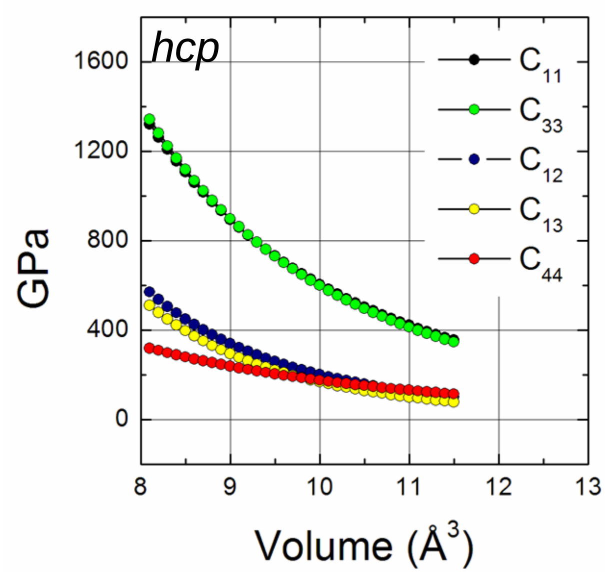

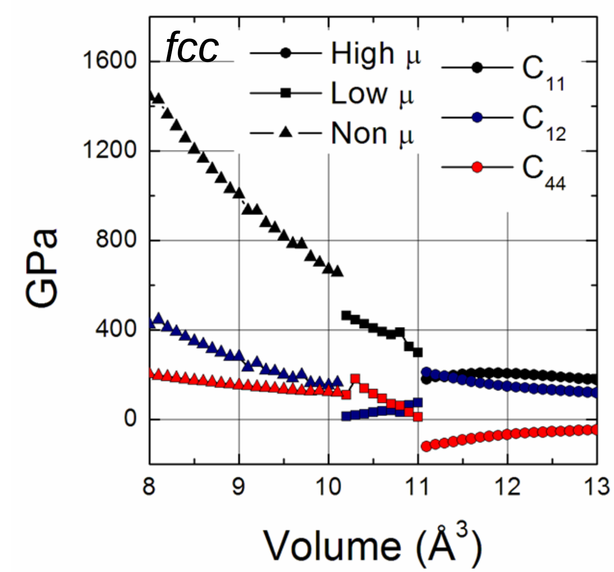

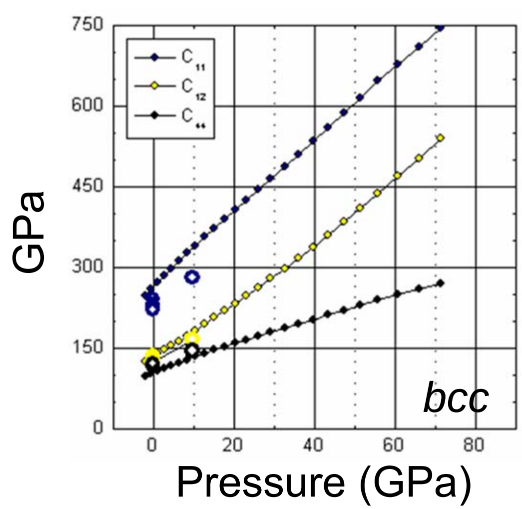

- *bcc* elastic constants compare well with experiment (C_{11} a bit high)
- little experimental data for *hcp* and *fcc*
- *fcc* shows instability in the high and low spin cases